Geomorphology 306 (2018) 28–39

Contents lists available at ScienceDirect

Geomorphology

journal homepage: www.elsevier.com/locate/geomorph

Influence of declining mean annual rainfall on the behavior and yield of sediment and particulate organic carbon from tropical watersheds

Ayron M. Strauch [a,*], Richard A. MacKenzie [b], Christian P. Giardina [b], Gregory L. Bruland [c]

[a] University of Hawai'i, Mānoa, Department of Natural Resources and Environmental Management, 1910 East-West Road, Sherman 101, Honolulu, HI 96822, United States
[b] Institute of Pacific Islands Forestry, Pacific Southwest Research Station, USDA Forest Service, 60 Nowelo Street, Hilo, HI 96720, United States
[c] Department of Biology and Natural Resources, Principia College, 1 Maybeck Place, Elsah, IL 62028, United States

ARTICLE INFO

Article history:
Received 16 May 2017
Received in revised form 21 December 2017
Accepted 22 December 2017
Available online 04 January 2018

Keywords:
Climate change
Sediment
Particulate organic carbon
Runoff
Tropical watershed
Hawai'i

ABSTRACT

The capacity to forecast climate and land-use driven changes to runoff, soil erosion and sediment transport in the tropics is hindered by a lack of long-term data sets and model study systems. To address these issues we utilized three watersheds characterized by similar shape, geology, soils, vegetation cover, and land use arranged across a 900 mm gradient in mean annual rainfall (MAR). Using this space-for-time design, we quantified suspended sediment (*SS*) and particulate organic carbon (POC) export over 18 months to examine how large-scale climate trends (MAR) affect sediment supply and delivery patterns (hysteresis) in tropical watersheds. Average daily *SS* yield ranged from 0.128 to 0.618 t km^{-2} while average daily POC ranged from 0.002 to 0.018 t km^{-2}. For the largest storm events, we found that sediment delivery exhibited similar clockwise hysteresis patterns among the watersheds, with no significant differences in the similarity function between watershed pairs, indicating that: (1) in-stream and near-stream sediment sources drive sediment flux; and (2) the shape and timing of hysteresis is not affected by MAR. With declining MAR, the ratio of runoff to baseflow and inter-storm length between pulse events both increased. Despite increases in daily rainfall and the number of days with large rainfall events increasing with MAR, there was a decline in daily *SS* yield possibly due to the exhaustion of sediment supply by frequent runoff events in high MAR watersheds. By contrast, mean daily POC yield increased with increasing MAR, possibly as a result of increased soil organic matter decomposition, greater biomass, or increased carbon availability in higher MAR watersheds. We compared results to modeled values using the Load Estimator (LOADEST) FORTRAN model, confirming the negative relationship between MAR and sediment yield. However, because of its dependency on mean daily flow, LOADEST tended to under predict sediment yield, a result of its poor ability to capture the high variability in tropical streamflow. Taken together, results indicate that declines in MAR can have contrasting effects on hydrological processes in tropical watersheds, with consequences for instream ecology, downstream water users, and nearshore habitat.

1. Introduction

The transport of sediment by rivers and streams plays a small, but globally important role in the biogeochemical cycling of carbon and nutrients, while locally influencing the functioning of watersheds and the health of near-shore environments (Syvitski et al., 2003). Tropical rivers account for nearly 60% of global water discharge, 40% of global sediment load, and 17–35% of global riverine particulate organic carbon (POC) inputs to oceans (Syvitski et al., 2014), but the functioning of these hydrological systems are greatly understudied compared to those in temperate regions (Lyons et al., 2002; Wohl et al., 2012). On tropical islands, a majority of suspended sediment is produced during infrequent, short-duration, high runoff events (Doty et al., 1981). Such events account for only a small portion of the annual hydrograph but appear to be responsible for the majority of annual sediment transport. Further, nearly all Hawaiian watersheds are characterized as small and mountainous, which are increasingly being recognized as important sources of POC to the ocean (Komada et al., 2004; Fang et al., 2015; MacKenzie et al., 2017).

Rainfall on high islands is greatly influenced by the orographic effect. As warm, moist trade wind-driven air is pushed upward by mountains, the rising air cools, and moisture condenses into rainfall and fog drip. Accumulated surface runoff carves steep gulches, channeling sediment eroded from the landscape into streams (Holz et al., 2015). Climate-related changes to the magnitude and frequency of rainfall events (Muller et al., 2011; Timm et al., 2013; Chen and Chu, 2014) are expected to impact the hydrology of tropical watersheds (Parry et al., 2007; Strauch et al., 2015) including shifts in the amount and timing of surface water runoff delivered to streams and near-shore regions (Barlage et al., 2002; Webster et al., 2005). Increases in air and ocean temperatures for the Eastern Pacific (Ruosteenoja et al., 2003), coupled

* Corresponding author.
E-mail address: astrauch@hawaii.edu (A.M. Strauch).

https://doi.org/10.1016/j.geomorph.2017.12.030
0169-555X/

with decreased rainfall (Mimura et al., 2007; Timm et al., 2011), have already impacted the distribution, frequency, and intensity of both rainfall (Chu and Chen, 2005) and streamflow in Hawai'i (Oki, 2004). Increasing periods of drought (McGregor and Nieuwolt, 1998; Chu et al., 2010) will reduce the capacity of streams and underlying aquifers to support community and ecosystem needs (Meehl, 1996; Strauch et al., 2017). In Hawaiʻi, the current trend of a diminishing vertical lapse rate is expected to result in steadily drier conditions in many regions, which will result in reduced groundwater recharge (Giambelluca et al., 2008) and contributions to base flows (Oki, 2004). Both wet season (November to April) and dry season (May to October) rainfall in Hawaiʻi has declined over the last century (Frazier and Giambelluca, 2016) and are expected to continue to decline (Timm et al., 2011). Until the 1970s, temperature and rainfall patterns were strongly coupled with the Pacific Decadal Oscillation. However, there has been a steady increase in temperature since the 1970s (Giambelluca et al., 2008), an increase in trade wind inversion frequency (Cao et al., 2007) and a decline in rainfall (Frazier and Giambelluca, 2016) resulting in an increase in drought probability in Hawaiʻi (Chu et al., 2010).

While declines in streamflow would be expected to result in less sediment export from watersheds, discharge and sediment transport are not linearly correlated, with most sediment exported during short duration pulse events in the tropics (Presley et al., 2008). Future trends in soil loss from tropical islands are difficult to predict because of a lack of long-term datasets. Previous research dealing with sediment transport in tropical islands has focused on single watersheds (Jennerjahn et al., 2004; Victor et al., 2006; Polyakov et al., 2007), the effect of major (hurricane) rainfall events (Yuan et al., 2015), non-point source pollution across a highly urbanized region (Freeman and Fox, 1995; Grigg, 1995), or limited sampling frequency (Augustijn et al., 2011). Surface runoff and sediment transport are largely driven by the frequency and intensity of rainfall (López-Tarazón et al., 2010), when rainfall exceeds the infiltration rate of soil (by Hortonian flow) or when soils are fully saturated (by saturation excess flow). Soil loss integrates watershed management and land use, indicating the loss of mineral nutrients, organic matter, and soil moisture, as well as the breakdown of soil structure (Brooks et al., 2013) or soil composition (Kleinman et al., 2006; Strauch et al., 2016) and the availability of rock-derived nutrients (Vitousek et al., 2003). In the tropics, intense rainfall events and steep topographic gradients accelerate the movement of water from sheetflows to rills that have enough energy to dislodge soil particles from the soil surface (Torri et al., 1987). Rills move sediment and organic material quickly into streams with hydrologic processes occurring on the order of minutes to hours (Syvitski et al., 2014; Strauch, 2017). However, substantial dilution or reduced sediment supply often take place in wet tropical forests resulting in the decline of the concentration of soil-derived solutes or particulates (Shanley et al., 2011). This contrasts with continental systems, where variability occurs at time scales of days to months (Brasington and Richards, 2000). Thus new model systems are needed to improve our understanding of climate change effects on the functioning of tropical watersheds (Vitousek, 1995; Allen and Ingram, 2002).

A few modeling efforts have examined streamflow in tropical island environments to predict how flow and sediment yield in highly variable and inherently unpredictable systems will respond to climate change (Cuo et al., 2006; Safeeq and Fares, 2012). In most cases, models have under-estimated sediment delivery from tropical island watersheds, highlighting the need to improve our empirical understanding of sediment dynamics (Calhoun and Fletcher III, 1999). Quantifying how rapidly changing hydrographs mobilize sediment can improve estimates of sediment export (Strauch, 2017). Characterizing relationships between sediment concentration and discharge (i.e., hysteresis) is used to understand sediment sources and responses to runoff within a watershed. However, quantifying hysteresis is challenging because patterns are generally non-linear (Williams, 1989) and traditional sampling programs are inadequate for identifying temporal variation in sediment concentration (Walling, 1977). Because of financial and logistical constraints to conducting extensive point sampling, in situ optical turbidimeters are used to improve temporal accuracy of suspended sediment estimates (Stock and Tribble, 2010).

To improve our understanding of how large-scale climate (MAR) affects sediment transport patterns, we deployed optical turbidimeters in three watersheds adjacent to stream gaging stations (Table 1) on the Island of Hawaiʻi to monitor the concentration of suspended sediment (*SS*), examine temporal variations in sediment concentrations, and to calculate *SS* and particulate organic carbon (POC) yield. These three watersheds provide a unique study system where mean annual rainfall (MAR) varies by 900 mm within a small spatial scale (10.5 km), while minimizing variation in other factors that influence soil erosion (e.g., geology, land use, land cover).

The specific objectives of this study were to: (1) quantify *SS* and POC over time to compare broad trends among watersheds with varying MAR; (2) examine *SS* hysteresis patterns during large flood events to determine if sediment sources and sediment transport behavior varied among watersheds; and (3) compare *SS* and POC export values to modeled values to determine the usefulness of the U.S. Geological Survey Load Estimator (LOADEST) Fortran export model for tropical watersheds. Quantifying changes in *SS* or POC could provide insights into hydrological responses to climate change (Campbell et al., 2009). Previous efforts found that declines in MAR led to (1) increased lengths of drought and a decrease in the frequency of runoff pulses (Strauch et al., 2015); (2) increased variability of streamflow (Strauch et al., 2017); and (3) increased concentrations of fecal bacteria in runoff pulses (Strauch et al., 2014). We hypothesized that with small declines in MAR there would be an increase in the mobilization of sediment and the yield of *SS* during runoff pulses. We expected repeated frequent runoff events in the highest MAR watershed would lead to an exhaustion of sediment supply. Suspended sediment and POC yields were then compared to estimates from other watersheds across the Hawaiian Islands of differing ages to test if island age influences the availability of sediment.

2. Methods

2.1. Station locations

We monitored three watersheds on the windward slope of the Island of Hawaiʻi (Fig. 1) beginning in September 2011 ('Uma'uma and Manowai'ōpae) or in September 2012 (Pāhale). Watersheds did not vary with respect to land use/land cover: intact forest above 500 m elevation with similar closed-canopy composition in the upper elevations (above 700 m, >85% of stand basal area dominated by one canopy

Table 1
Station elevation (m), upstream catchment area (km^2), upstream mean annual rainfall (mm), mean catchment slope (%), median flow ($m^3\ s^{-1}$), ratio of runoff to baseflow (runoff:baseflow), flow coefficient of variation (CV), mean daily suspended sediment (*SS*) load ($t\ d^{-1}$) and daily SS yield ($t\ km^{-2}\ d^{-1}$), and mean daily particulate organic carbon (POC) load ($t\ d^{-1}$) and daily POC yield ($t\ km^{-2}\ d^{-1}$), from three watersheds on the Island of Hawaiʻi for the period September 2012 to April 2014.

	'Uma'uma	Manowai'ōpae	Pāhale
Station elevation (m)	490	470	510
Catchment (km^2)	74.427	3.836	10.143
Mean annual rainfall (mm)	4906	4689	4026
Mean catchment slope (%)	15.8	13.8	12.0
Median flow ($m^3\ s^{-1}$)	0.337	0.002	0
Runoff: baseflow	3.27	3.79	13.31
Flow CV	4.89	5.32	5.5
Mean (±SE) daily *SS* load ($t\ d^{-1}$)	9.55 (3.24)	1.34 (0.51)	6.27 (2.68)
Mean (±SE) daily *SS* yield ($t\ km^{-2}\ d^{-1}$)	0.128 (0.04)	0.348 (0.13)	0.618 (0.26)
Mean (±SE) daily POC load ($t\ d^{-1}$)	1.33 (0.36)	0.02 (0.01)	0.03 (0.01)
Mean (±SE) daily POC yield ($t\ km^{-2}\ d^{-1}$)	0.018 (0.005)	0.008 (0.003)	0.002 (0.001)

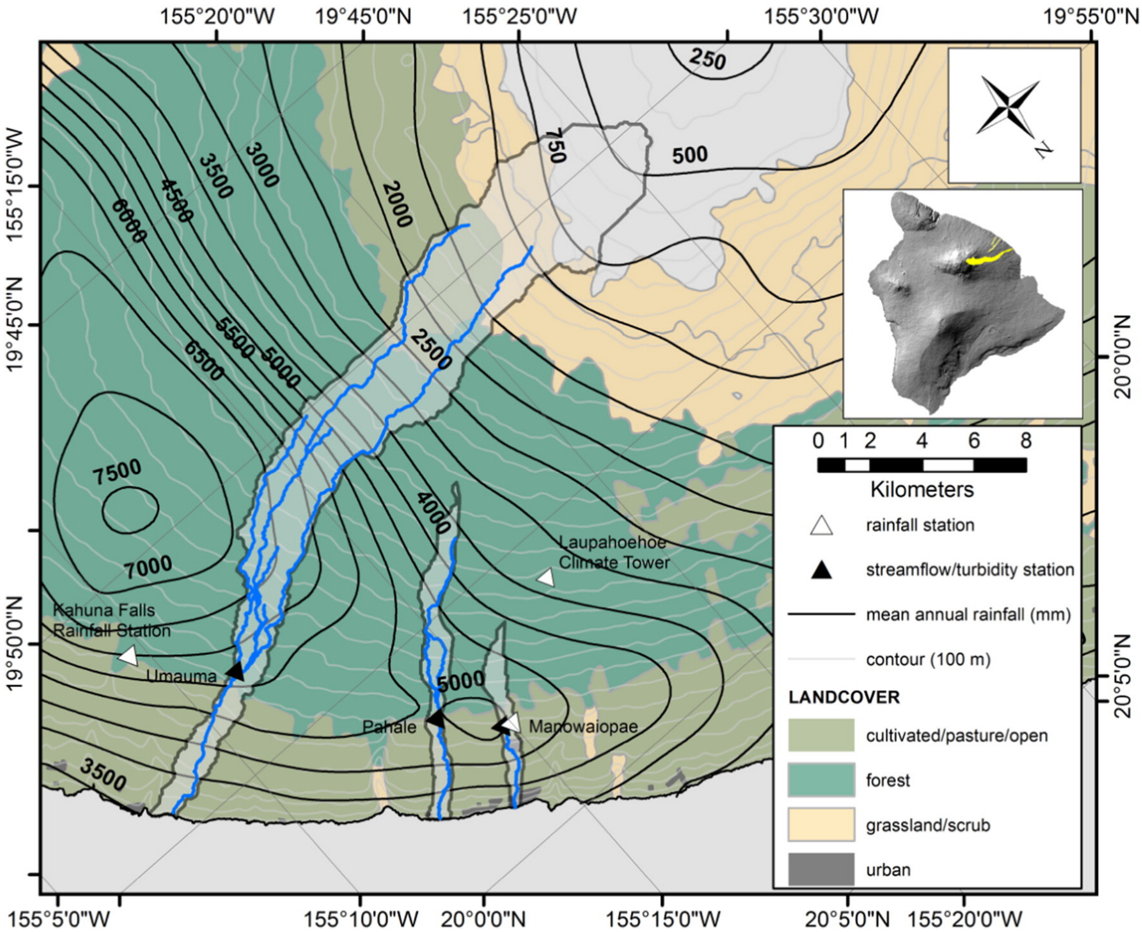

Fig. 1. Map of watersheds, gaging stations, rainfall stations, and land-cover on windward Hawai'i Island.

species and one mid-story species); pasture/row crop agriculture below 500 m elevation. Stations were located above anthropogenic modifications to the landscape to isolate the consequences of changing climate as depicted with MAR. The bedload transport rate was not measured, but field observations suggest that bedload is a minor component of the total sediment load on young lava flows. Further, Presley et al. (2008) found Hawaiian streams to be well mixed during high flow events. River channels had steep slopes (8–15°) and are primarily composed of bedrock lava or large boulders, with some cobble and gravel intermixed and only small pockets of sand or silt. Land-cover data were analyzed using the U.S. Geological Survey (USGS) Hawaii Gap Analysis Program satellite data products with land-use or ecosystem values based on 30 m resolution pixels available through the State of Hawai'i Office of Planning (http://planning.hawaii.gov/gis/download-gis-data/). Underlying geology and soils were identified using USGS geology and Natural Resources Conservation Service maps (Sherrod et al., 2007; USDA, 2008). All soils are similarly aged (11–300 ky) Hydraudands (taxanomic classes of Hydrous, Ferrihydritic, and Isothermic Acrudoxic) of the same volcanic origin (Mauna Kea), consistent across watersheds with Hamakua Volcanics underlying Laupāhoehoe Volcanics (USDA, 2008). Modeled upstream soil organic carbon content (up to a depth of 1 m) was analyzed for each watershed using data from Selmants et al. (2017). Mean (±SD) soil organic carbon was 25.04 (±9.10) kg C m^{-2} for Uma'uma, 36.04 kg C m^{-2} for Manowai'ōpae, and 29.29 (±11.62) kg C m^{-2} for Pāhale.

2.2. Rainfall

Watershed MAR was calculated based on Giambelluca et al. (2013) as described in Strauch et al. (2015). Rainfall was measured at Manowai'ōpae (490 m a.s.l.) using Onset® data logging rain gage (MAN-RG3) and south of 'Uma'uma at Kahuna Falls (GHCND:USC00512595; Kahuna Falls 138.2; elevation 423.7 m a.s.l.). Missing data (14.1%) between 1 October 2011 and 30 April 2014 at Kahuna Falls were gap filled using a nearby station (GHCND:US1HIHI0014; Honomū 2.8 SW) with a strong linear relationship in total daily rainfall ($R^2 = 0.91$). Rainfall at the Pāhale station was determined using measured values (from 21 Oct 2011 to 4 May 2012) and the remainder of the data estimated based on distance weighted ratios using the previously mentioned stations. The total number of rainfall events larger than 50 mm d^{-1} and 100 mm d^{-1}, the number of antecedent dry days (ADD; the number of days with cumulative rainfall <10 mm d^{-1}), and the total cumulative 5 d rainfall (RF_{5d}), were calculated for each station. To examine the relationship between soil moisture, rainfall, and runoff, we examined mean soil moisture from the 0–30 cm interval depth at the Laupāhoehoe climate station near the Manowai'ōpae Watershed.

2.3. Streamflow

Streams were classified as perennial based on Parham et al. (2008), but zero flow conditions were occasionally observed in Pāhale and Manowai'ōpae streams. In young tropical islands, even perennial streamflows are dominated by runoff and shallow groundwater, with intermittent flows common during dry periods because highly porous geology limits bank-storage. Instantaneous flow was measured at 15 min intervals. Stage at Pāhale was measured using non-vented HOBO® U20 depth sensors (Onset, Bourne, MA) corrected for changes in barometric pressure. Stage in 'Uma'uma and Manowai'ōpae streams were measured by vented WaterLOG® Model H-312 (Design Analysis

Associates Inc., Logan, UT) depth sensors with data stored in CR295X data loggers (Campbell Scientific Inc., Logan, UT). Flow was then calculated for each stream as reported in Strauch et al. (2015). Fifteen minute interval data were used to characterize streamflow regimes and examine sediment hysteresis (see Olden and Poff, 2003).

2.4. Turbidity and suspended sediment measurements

Turbidity was measured at 15 min intervals in the 'Uma'uma and Manowai'ōpae rivers using a DTS-12 Turbidity Sensor (Forestry Technology Systems Inc., Victoria, BC, Canada). In September 2012, an Analite NEP495 Turbidity-Temperature Probe (McVan Instruments, Victoria, Australia) was installed at Pāhale. Each sensor was self-cleaning but bi-weekly visits to the sites confirmed sensors remained free of algae and debris. Each turbidity sensor was housed in a 1.22 m floating boom facing downstream that kept the probe submerged 10 cm below the water surface during all but the most extreme flows, during which the probe was submerged to a greater depth.

To convert instantaneous turbidity measurements to total suspended sediment concentration (*SS*), grab samples were taken using acid-washed 500 mL HDPE bottles from as close to the thalweg as possible at least 10 cm below the surface across the range of encountered streamflows and turbidity measurements. At high flows, Hawaiian streams are well mixed, resulting in minimal differences between point samples and discharge-weighted samples (Presley et al., 2008). Samples were placed on ice and returned to the lab where 100 mL subsamples were filtered through pre-combusted 47 mm diameter, 0.7 μm pore Watman GF/F glassfiber filter using vacuum filtration to determine *SS*. We then graphed turbidity as measured in Nephelometric Turbidity Units (NTU) and suspended sediment (mg L^{-1}) on log-log scales to examine relationships between turbidity and *SS* (Fig. 2). A log-log regression model was generated based on ordinary least-squares to estimate *SS* using measured turbidity values. Daily sediment discharge was generated by multiplying each converted *SS* value (mg L^{-1}) by streamflow (L s^{-1}) to estimate sediment flux (mg s^{-1}) and by 900 s (15 min) to estimate *SS* load for each interval. Non-linear regression equations between daily suspended sediment discharge and mean daily flow were used to examine broader trends between watersheds. Total daily sediment discharge and mean daily flow for additional locations elsewhere in Hawai'i were provided by the USGS using the National Water Information System.

2.5. Carbon measurements

Samples for correlating turbidity (NTU) to *SS* (mg L^{-1}) were also analyzed for particulate organic carbon (POC) at the UH Hilo Analytical Lab. A CHN analyzer (Costech Analytical Technologies, Valencia, CA) was used to analyze filtered samples for percent organic carbon. Results were multiplied by *SS* to get POC (mg L^{-1}). A linear regression model between turbidity and POC was generated similar to that with *SS*

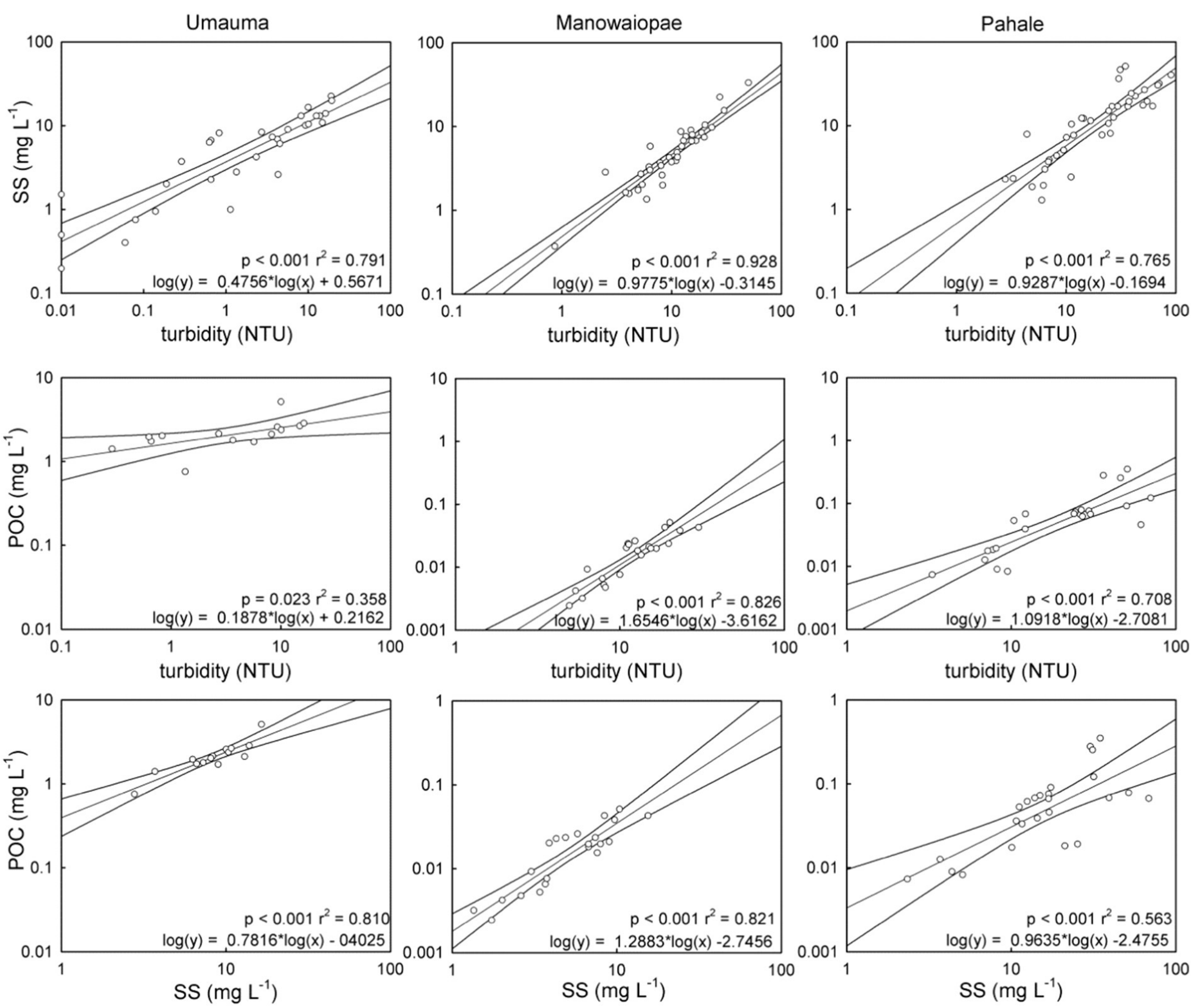

Fig. 2. Measured suspended sediment (SS; mg L^{-1}) vs. turbidity (NTU) (top); measured particulate organic carbon (POC; mg L^{-1}) vs turbidity (middle); and measured POC vs measured SS (bottom) and the log-log linear regression model, coefficient of determination, and significance value for three watersheds on the Island of Hawai'i with 95% confidence intervals.

(Fig. 2). Estimated POC (mg C L^{-1}) was multiplied by streamflow (L s^{-1}) to estimate carbon flux (mg C s^{-1}) and by 900 s (15 min) to estimate POC load for each interval. Total daily POC discharge was then estimated by summing values for each station.

2.6. LOADEST Fortran model

To compare measured *SS* and POC values with modeled values, daily *SS* and POC loads were generated using the USGS Load Estimator (LOADEST) Fortran model (Runkel et al., 2004). The LOADEST model is a multiple-regression based Adjusted Maximum Likelihood Estimation (AMLE) model that uses measured concentration values to calibrate a regression and then generates a constituent load using mean daily flow (MDF). The model requires flow values in $ft^3\ s^{-1}$ and concentration in mg L^{-1}. Model calibration used at least 21 *SS* or POC (in mg L^{-1}) point samples paired with instantaneous streamflow values. Once calibrated for each stream, LOADEST then used mean daily flow to estimate daily *SS* and POC load. When streamflow was extremely low (<0.001 $ft^3\ s^{-1}$, $2.831 \times 10^{-5}\ m^3\ s^{-1}$), a value of 0.001 $ft^3\ s^{-1}$ ($2.831 \times 10^{-5}\ m^3\ s^{-1}$) was used because LOADEST requires nonzero flow values. The models used to estimate loads for individual stations varied in terms of coefficients and estimates of log load (Zhu and Reed, 2012), and the program was set to permit LOADEST to select the best of nine models based on Akaike's Information Criterion (Runkel et al., 2004). LOADEST output complications, including retransformation bias, data censoring, and non-normality were greatly reduced using AMLE and the highest value for the Schwarz Posterior Probability Criterion (SPCC). The estimated loads and their standard errors were used to develop 95% confidence intervals. The model's performance was examined by reviewing its output, such as the partial load factor (PLF) between calibrated and estimated concentration exceedance values, concentration load bias (Bp), the Nash-Sutcliffe Efficiency (NSE) coefficient (Stenback et al., 2011), AMLE's coefficient of determination (R^2) values and residuals (model error). The Nash-Sutcliffe Efficiency coefficient ranges from -∞ to 1 with values above zero indicating model predictions are more accurate than the mean of the observed data. Models with Bp exceeding acceptable limits (−25% to +25%) were rejected and recalibration was accomplished by eliminating values (<25% of data) based on the distribution of residuals from the actual versus the predicted biplot. Mean daily *SS* and POC loads were then estimated for each of the three streams using the formulas with the lowest AIC values. Daily values were then summed by month and year.

2.7. Data analysis

Mean daily flow was separated into runoff and baseflow for each day using a baseflow separation procedure based on a recursive digital filter (Lim et al., 2005). The percentage of daily runoff to daily total flow was calculated for the period of record as was the ratio of daily runoff to total daily flow. Total watershed area co-varied with MAR, but calculations of sediment yield were normalized by catchment area. Daily mean *SS* (mg L^{-1}), total daily *SS* load (t d^{-1}), daily sediment yield (t $km^{-2}\ d^{-1}$), and monthly yield (t $km^{-2}\ month^{-1}$) were calculated and the logarithmic curve of best fit was used to describe the relationship between daily *SS* load and MDF for each watershed. Mean monthly *SS* yield was analyzed using a repeated measures Analysis of Variance (RM-ANOVA).

We examined hysteresis patterns to better understand the relationship between *SS* and streamflow (*Q*) among watersheds for the 14 largest flood events (see Gellis, 2013 for a review of hysteresis patterns). Tropical stream hydrographs are highly variable, and separating out individual flood events is made challenging by the frequent occurrence of intense, short-duration rainfall events that temporarily increase shallow groundwater contributions to streamflow. Individual flood events were selected based on maximum flows while maintaining at least 24 h between peak events. If events were bimodal, only the first peak of the event was analyzed. Because of differences in watershed size, maximum peak flows differed among watersheds and both parameters were normalized as the value relative to the maximum *Q* or *SS* for the event as detailed in Fang et al. (2015). Because of the relatively close proximity of the watersheds, rainfall events generally resulted in flood events of some magnitude for each watershed at approximately the same time, although in one event only two of the three watersheds displayed a noticeable response to rainfall and this event was eliminated from further analysis. To test for differences in the total hysteresis behavior of individual flood events between pairs of watersheds the unitless similarity function (SF) was used as described in Smith and Dragovich (2009). The SF function uses line segments and the angle generated between subsequent line segments connecting points in a biplot of measured values of *SS* (y-axis) and discharge (x-axis) for two consecutive time steps (see Figure 5c). The SF function is determined by the sum of two ratios for paired watersheds (Eq. 1) for a given flood event:

$$SF = A_R + L_R \tag{1}$$

The first ratio (A_R) is the mean angle for the flood event for watershed one ($W1$) divided by the mean angle for the same flood event for watershed two ($W2$) as depicted in Eq. (2). The second ratio (L_R) is the mean value of the product of individual line segments length (L_t) with their corresponding angle (A_t) for watershed one ($W1$) divided by the product of line segments with their corresponding angle for watershed two ($W2$) as depicted in Eq. (3):

$$A_R = \frac{mean\ A_{W1}}{mean\ A_{W2}} \tag{2}$$

$$L_R = \frac{\left[\sum_{t=1}^{N} \frac{L_{W1_t}}{L_{W2_t}} \frac{A_{W1_t}}{A_{W2_t}}\right]}{N} \tag{3}$$

Table 2
Rainfall (mm), number of days of rainfall exceeding 50 mm (>50 mm d^{-1}), number of days of rainfall exceeding 100 mm (>100 mm d^{-1}), the average 5 d rainfall (RF_{5d}, mm) and the maximum RF_{5d} for each given time interval for three rainfall stations on the Island of Hawai'i. CY = calendar year.

Statistic	Time interval	Kahuna Falls	Manowai'ōpae	Pāhale
Rainfall (mm)	CY 2012	4205	1933	1953
Rainfall (mm)	CY 2013	4078	3761	3648
>50 mm d^{-1}	9/1/12 to 4/30/14	48	39	35
>100 mm d^{-1}	9/1/12 to 4/30/14	17	11	12
Mean RF_{5d} (mm)	9/1/12 to 4/30/14	64.73	53.79	51.91
Max RF_{5d} (mm)	9/1/12 to 4/30/14	667.0	946.4	895.9

Table 3
Spearman rank non-parametric correlations between the 5 d cumulative rainfall (RF_{5d}; mm), total rainfall (RF) on the day of the runoff event (mm) or antecedent dry days (ADD) and maximum suspended sediment yield SS_{max} or maximum streamflow (Q_{max}; $m^3\ s^{-1}$) for the 13 largest flood events between September 2012 and April 2014 for three streams on the Island of Hawai'i.

	RF_{5d} (mm)	RF (mm)	ADD (d)
'Uma'uma			
SS_{max}	0.66*	0.64*	−0.29
Q_{max}	0.63*	0.44	−0.31
Manowai'ōpae			
SS_{max}	0.68*	0.57*	−0.72**
Q_{max}	0.55	0.56	−0.60*
Pāhale			
SS_{max}	0.55	0.55	−0.23
Q_{max}	0.61*	0.75**	−0.21

* $p < 0.05$.
** $p < 0.01$.

Table 4
Spearman non-parametric correlations between suspended sediment (*SS*) discharge (t d^{-1}) or particulate organic carbon (POC) discharge (t d^{-1}), versus the ratio of maximum daily streamflow (Q_{max}) to the period of record mean daily flow (MDF) from 1 September 2012 to 1 April 2014 (580 days) for three watersheds on the Island of Hawai'i.

	Uma'uma	Manowai'ōpae	Pāhale
	Q_{max}/MDF	Q_{max}/MDF	Q_{max}/MDF
SS discharge (t d^{-1})	0.64***	0.75***	0.80***
POC discharge (t d^{-1})	0.65***	0.74***	0.80***

*** $p < 0.001$.

Each line segment length (L_t) is calculated as in Eq. 4 and line angles (A_t) calculated (in radians) as in Eq. (5) for each consecutive sampling interval for an entire flood event:

$$Line\ Length\ (L_t) = \left[(SS_{t+1} - SS_t)^2 + (Q_{t+1} - Q_t)^2\right]^{0.5} \quad (4)$$

$$Line\ Angle\ (A_t) = \tan^{-1}\left(\frac{|Q_{t+1} - Q_t|}{|SS_{t+1} - SS_t|}\right) \quad (5)$$

The closer each ratio is to 1, the closer either A_R or L_R, and therefore the hysteresis behavior, between paired watersheds for a single flood event. A SF value was determined for each flood event between each pair of watersheds. A one-sample *t*-test was used to test the hypothesis that a watershed pair SF was significantly different from 2 for all events (the value if both A_R and L_R are exactly equal representing equal functions). The differences in the mean L_t and mean A_t for each watershed were also compared using a one-way Analysis of Variance (ANOVA). For all tests, we used $\alpha = 0.05$.

Relationships between antecedent rainfall conditions (RF, RF_{5d} or ADD) and maximum sediment yield (SS_{max}) or maximum streamflow (Q_{max}) were examined by Spearman non-parametric correlation. Using a step-wise regression model, we tested factors that may have a significant effect on daily *SS* discharge including mean soil moisture (%), total daily rainfall, RF_{5d}, mean flow, and max flow at the Manowai'ōpae Station.

3. Results

3.1. Rainfall, runoff, and streamflow

Total rainfall was consistently greater at the wet site (Kahuna Falls) than either dry sites (Manowai'ōpae or Pāhale), with 2012 being slightly wetter at the wet site but substantially drier at the dry sites compared to 2013 (Table 2). From 1 September 2012 to 30 April 2014, there were approximately 23% more of rainfall events >50 mm d^{-1} and approximately 50% more rainfall events >100 mm d^{-1} at the Kahuna Falls station than at the Manowai'ōpae station. Soil moisture at the Laupāhoehoe Climate Station was not significantly related to RF or RF_{5d} at these stations.

As expected, streamflow statistics followed the general trend of decreasing MAR (Table 1): mean daily flow (MDF) was greatest for 'Uma'uma, followed by Pāhale and Manowai'ōpae, while streamflow CV increased with decreasing MAR. From September 2012 to April 2014, mean daily runoff represented 76.6% of MDF for 'Uma'uma, 80.9% of MDF for Manowai'ōpae, and 81.1% of MDF for Pāhale. For the largest storm events, there were significant correlations between RF_{5d} and Q_{max} at the 'Uma'uma and Pāhale stations while RF was positively correlated to SS_{max} at Manowai'ōpae and 'Uma'uma stations, while RF was positively correlated to Q_{max} at Pāhale (Table 3). Antecedent dry days was significantly negatively correlated to both SS_{max} and Q_{max} in Manowai'ōpae, but not in the other two streams. There were also significant correlations between the relative size of the maximum daily flow (Q_{max}/MDF) and daily *SS* or POC discharge for each stream (Table 4).

3.2. Daily and monthly trends in sediment and particulate organic carbon export

Mean daily *SS* load increased with MDF for all streams (Fig. 3) and daily *SS* yield decreased with MAR reflecting the increasing runoff to baseflow ratio with declining MAR (Table 1). For the calendar year 2013, total *SS* yield in Pāhale was 324 t km^{-2}, followed by 172 t km^{-2} in Manowai'ōpae and 65 t km^{-2} in 'Uma'uma. By contrast, mean daily POC load and daily POC yield increased with increasing MAR (Table 1). For the calendar year 2013, total POC yield in Pāhale was 1.14 t km^{-2}, followed by 3.94 t km^{-2} in Manowai'ōpae and 8.57 t km^{-2} in 'Uma'uma.

In the stepwise regression model, soil moisture ($\beta = -26.13$, $F = 35.67$, $R^2 = 0.84$), MDF ($\beta = 18.48$, $F = 79.28$, $R^2 = 0.83$), and Q_{max} ($\beta = -2.991$, $F = 77.55$, $R^2 = 0.81$) were significant controls on *SS* discharge in Manowai'ōpae (but not total daily rainfall or RF_{5d}), producing a significant ($F = 961.15$, $p < 0.001$) model that accounted for much of the variability in the data (adj. $R^2 = 0.84$).

Maximum monthly sediment yield was 26.3 t km^{-2} for 'Uma'uma, 110.7 t km^{-2} for Manowai'ōpae, and 223.7 t km^{-2} for Pāhale (Fig. 4) but mean monthly *SS* was not significantly different between watersheds ($\chi^2 = 4.105$, $p = 0.13$). Sediment yield during the wet season (November to April), was greater in 2014 than in 2013 for each watershed and 10–100 times greater than dry season sediment yield for each watershed.

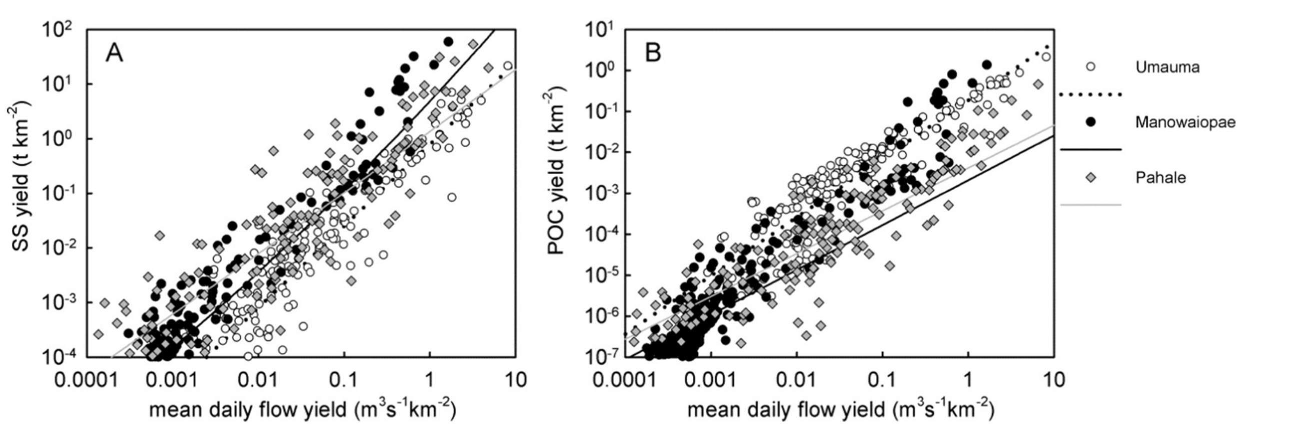

Fig. 3. (A) Daily suspended sediment (SS) yield (t km^{-2}) and (B) particulate organic carbon (POC) yield (t km^{-2}) versus mean daily flow yield ($m^3\ s^{-1}\ km^{-2}$) and the line of best fit from least squares regression modeling for three streams on the Island of Hawai'i.

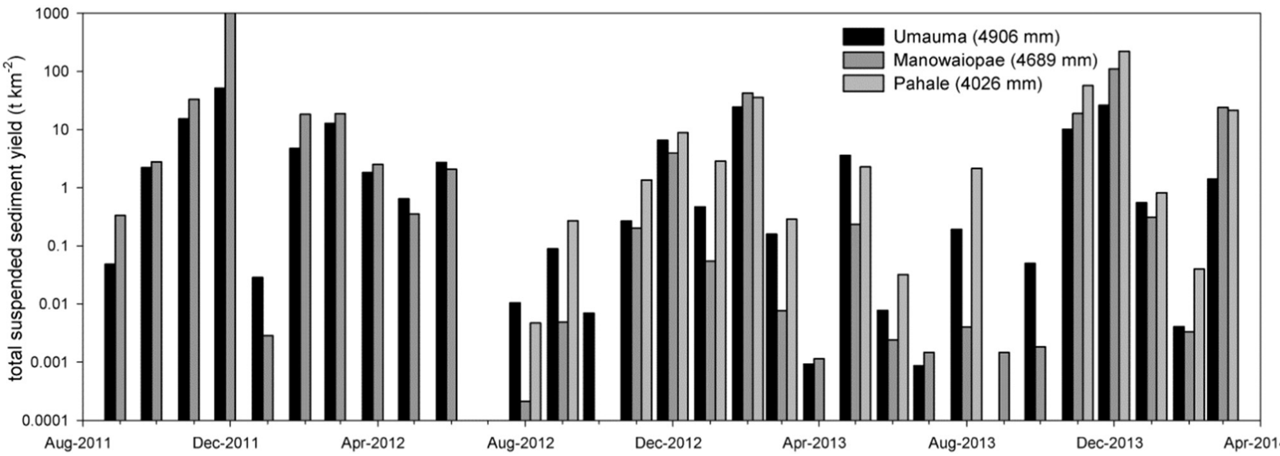

Fig. 4. Monthly total suspended sediment yield from three watersheds (by mean annual rainfall) on the Island of Hawai'i from September 2011 (Uma'uma and Manowai'ōpae) or September 2012 (Pāhale) to April 2014.

3.3. Patterns in suspended sediment during large storm events

Suspended sediment hysteresis patterns were examined for the 13 largest individual flood events (Table 5). Sediment hysteresis varied by flood event, but generally followed similar patterns at each station over time. All events for each watershed exhibited a clockwise pattern, with initial SS concentrations rising more rapidly than discharge and peaking prior to peak streamflow (Fig. 5). Mean ($\pm$SD) SF between 'Uma'uma and Manowai'ōpae was 2.075 ($\pm$0.771), between 'Uma'uma and Pāhale was 1.82 ($\pm$0.41), and between Manowai'ōpae and Pāhale was 1.78 ($\pm$0.52) and none were significantly different from 2.0. Descriptive statistics for normalized line segments and segment angles are provided in Table 6. While there was no significant difference in mean line segment among watersheds (ANOVA F = 0.77, df = 2, 39, p = 0.47), there was a significant difference in mean segment angle among watersheds (ANOVA F = 3.79, df = 2, 39, $p < 0.05$), probably as a result of vastly different quantities of water moving past the gaging station during high flow periods.

3.4. Comparison to model estimates of suspended sediment and total particulate carbon

Based on NSE and R^2, all LOADEST models produced reasonable relationships between estimated and measured concentrations for both *SS* and POC, although regression models varied in terms of load bias (Table 7). Modeled mean daily *SS* estimates for the period of record using LOADEST were 6.99 t d^{-1} for 'Uma'uma, 0.081 t d^{-1} for Manowai'ōpae, and 4.23 t d^{-1} for Pāhale, resulting in modeled mean daily *SS* yields of 0.094 t km^{-2} d^{-1} for 'Uma'uma, 0.021 t km^{-2} d^{-1} for Manowai'ōpae, and 0.417 t' km^{-2} d^{-1} for Pāhale. Estimates of annual POC yield were 40.8, 75.6%, and 68.8% lower than estimates using sub-daily turbidity and discharge measurements for 'Uma'uma, Manowai'ōpae, and Pāhale, respectively (Table 8).

4. Discussion

Sediment export is an increasingly appreciated factor in the decline of near-shore marine environments and coral reef ecosystems (IPCC, 2013). Rapid land-use change, continued expansion of non-native species and climate change are contributing to increased nutrient, sediment, and bacteria loads in tropical streams (Laws and Ferentinos, 2003; Strauch et al., 2014; Algeet-Abarquero et al., 2015). Despite substantial progress in science-based management of tropical watersheds, diverse threats continue to impact these systems, with implications for freshwater supply to industry and agriculture, tourism and human health, and ecosystem function (Milly et al., 2005; Wohl et al., 2012; Strauch et al., 2017). Changes in the duration, frequency, or intensity of rainfall events as well as longer inter-event dry periods are affecting runoff and the transport of sediment into streams. We found that declines in MAR were associated with changes in antecedent rainfall

Table 5
Flood and climate characteristics for the 13 largest flood events between September 2012 to April 2014 on the Island of Hawai'i: maximum streamflow (max *Q*; m^3 s^{-1}), maximum suspended sediment concentration (max *SS*; mg L^{-1}); daily rainfall (RF; mm) and cumulative 5 d rainfall (RF5d; mm).

Flood event	'Uma'uma station		Manowai'ōpae station		Pāhale station		Kahuna Falls climate station		Manowai'ōpae climate station	
	Max Q (m^3 s^{-1})	Max SS (mg L^{-1})	Max Q (m^3 s^{-1})	Max *SS* (mg L^{-1})	Max Q (m^3 s^{-1})	Max *SS* (mg L^{-1})	RF (mm)	RF5d (mm)	RF (mm)	RF5d (mm)
November 15, 2012	21.31	21.98	0.36	4.54	2.32	132.85	26.70	43.10	22.35	40.13
November 27, 2012	6.65	13.89	111.77	0.87	5.37	205.76	24.10	36.60	23.88	46.23
December 19, 2012	626.49	35.50	16.29	296.84	58.37	221.80	21.60	89.00	59.94	105.66
January 12, 2013	36.61	7.34	0.003	13.60	0.02	2.87	18.50	125.4	29.72	74.93
February 7, 2013	648.71	110.42	28.72	522.50	74.01	417.64	62.50	139.47	29.72	741.93
February 18, 2013	451.41	25.56	5.19	57.21	34.01	102.34	58.90	128.50	91.19	174.24
February 20, 2013	548.83	38.37	31.24	726.50	62.72	208.38	130.80	292.1	101.6	315.22
February 23, 2013	93.64	54.24	11.18	141.80	23.30	422.80	157.50	577.8	176.54	469.91
February 24, 2013	404.05	33.91	5.52	35.65	18.56	117.32	52.80	666.7	30.23	443.49
March 13, 2013	18.79	47.19	0.07	33.73	0.86	73.38	40.60	52.80	3.56	46.48
May 26, 2013	462.77	23.98	3.04	38.78	22.84	67.63	114.8	120.10	60.71	69.09
August 16, 2013	10.27	7.10	0.02	9.52	0.56	246.84	6.10	52.30	52.58	91.19
November 10, 2013	1432.9	95.08	12.40	1174.0	206.12	454.68	63.80	70.39	163.32	180.34
December 30, 2013	2409.5	79.17	26.45	1236.3	427.81	432.26	215.90	315.29	185.67	341.63

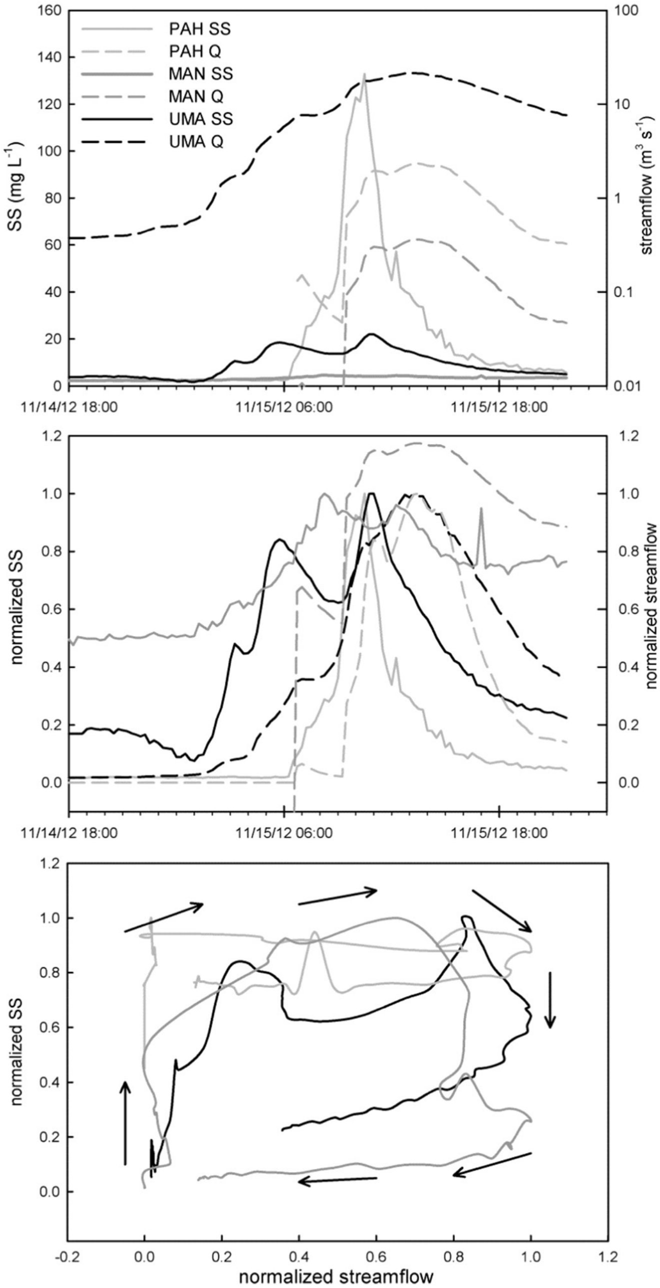

Fig. 5. (A) Suspended solids (SS; mg L^{-1}) and streamflow (Q; $m^3 s^{-1}$) for a typical rainfall-runoff event in November 2012 for the Pāhale (PAH), Manowai'ōpae (MAN), and Uma'uma (UMA) streams on the Island of Hawai'i; (B) SS and streamflow normalized by the maximum value at each station for the same event; (C) clockwise hysteresis patterns for the three gaging stations using normalized TSS and streamflow.

conditions, greater runoff relative to base flow and greater streamflow variation, leading to increased *SS* yield. Antecedent soil moisture is the primary influence on erosion during storm events, with wetter soils generally saturating quicker and producing overland flow sooner

Table 6
Descriptive statistics of the normalized suspended sediment hysteresis patterns for the 13 largest independent flood events among three watersheds on the Island of Hawai'i based on 15 min interval measurements.

	'Uma'uma	Manowai'ōpae	Pāhale
Mean (SD) line segment (unitless)	0.061 (0.021)	0.070 (0.043)	0.077 (0.028)
Mean (SD) segment angle (unitless)	0.825 (0.167)	0.696 (0.207)	0.880 (0.194)

Table 7
Concentration Load Bias (Bp), Load Nash-Sutcliffe Efficiency Index (NSE), and coefficient of determination (R^2) for the LOADEST model run used to estimate suspended sediment (*SS*) and particulate organic carbon (POC) loads for each station during calendar year 2013.

Watershed	Bp (%)	NSE	R^2
'Uma'uma			
SS	9.941	0.777	0.98
POC	2.928	0.877	0.97
Manowai'ōpae			
SS	−16.232	0.926	0.94
POC	−9.620	0.921	0.95
Pāhale			
SS	8.178	0.977	0.99
POC	−0.893	0.894	0.99

(Holz et al., 2015). However, the sediment supply in higher MAR watersheds may be exhausted by the higher frequency of intermediate runoff events. In watersheds with lower MAR, rainfall event frequency declines, with reductions in soil moisture resulting in a decrease in aggregate stability and thus an increase in soil available for erosion and transport (Holz et al., 2015), supporting the trends found in Strauch et al. (2014). We found no significant difference in the sediment-discharge hysteresis behavior of large storm events among watersheds suggesting that overall sediment sources did not vary among watersheds despite differences in watershed size and MAR, supporting the initial hypothesis that the underlying distribution of soils and sediment supply is generally similar among watersheds with nearly identical geologic origin, slope and shape.

4.1. Temporal fluctuations in sediment

The transport of sediment from the landscape varies substantially in response to rainfall, slope and parent material as a result of overland flow in narrow, steeply sloped watersheds (Strauch, 2017). In streams, storm events produce positive changes in flow rate, increasing the kinetic energy available to move sediment, as well as the energy available to re-suspend particles for further transport downstream (Kurashige, 1994; Millhous, 2003). Greater shear stress during periods of increasing discharge leads to greater than expected sediment in the rising limb of the hydrograph as new sediment sources are mobilized (Williams, 1989; Gellis, 2013). These flows transport more sediment than would be expected based on average flow values and are not captured in sediment models that use daily flow values (López-Tarazón et al., 2010). Rising and falling hydrographs or turbidity measurements represent different phases of sediment transport that are difficult to characterize using daily measurements (Lewis, 1996).

In contrast to large continental watersheds, which provided the basis for the development of LOADEST, tropical island streams are steeply sloped, drain smaller watersheds, and generally lack floodplains, resulting in unique sediment transport dynamics (Latrubesse et al., 2005). As a result, streamflow is flashier, scour is greater, and sediment sources are exhausted more rapidly (Victor et al., 2006). Measured loads for *SS* were 1.7–17 times and for POC 1.7–4.1 times greater than LOADEST modeled estimates. Models based on time scales of days often fail to capture runoff dynamics that occur at sub-daily scales, which can explain under-predictions of both flow and sediment (Calhoun and Fletcher III, 1999). The LOADEST model is dependent on mean daily flow, which poorly characterizes tropical watershed flows that can fluctuate by three orders of magnitude within a 24 h period (Strauch et al., 2015). Further, events lasting just a few hours can transport 90% of the sediment even while accounting for <2% of the measurement period (Doty et al., 1981). Clearly, models that provide increased temporal resolution of flow events will improve sediment load estimates for tropical watersheds.

Soil moisture proved to be a significant negative effect on sediment discharge, suggesting that increasing antecedent dry days (and thus

Table 8
Total suspended sediment (*SS*) load (t yr^{-1}), particulate organic carbon (POC) load (t yr^{-1}), *SS* yield (t km^{-2} yr^{-1}), and POC yield (t km^{-2} yr^{-1}) estimates using sub-daily flow and turbidity estimates or LOADEST model estimates using daily flow for three stations on the Island of Hawai'i during calendar year 2013.

Station	*SS* load estimated from sub-daily measurements (t yr^{-1})	*SS* load estimated from LOADEST (t yr^{-1})	*SS* yield estimated from sub-daily measurements (t km^{-2} yr^{-1})	*SS* yield estimated from LOADEST (t km^{-2} yr^{-1})	POC load estimated from sub-daily measurements (t yr^{-1})	POC load estimated from LOADEST (t yr^{-1})	POC yield estimated from sub-daily measurements (t km^{-2} yr^{-1})	POC yield estimated from LOADEST (t km^{-2} yr^{-1})
'Uma'uma	4849.34	2921.75	64.89	39.26	640.25	714.06	8.57	9.59
Manowai'ōpae	661.48	37.90	172.26	9.88	15.14	7.06	3.94	1.84
Pāhale	3288.89	1755.76	324.35	173.10	11.60	227.76	1.14	22.45

small reductions in soil moisture) can reduce the bonds holding soil particles together in aggregates and increasing sediment available to be transported during runoff events (Holz et al., 2015). However, the meteorological and hydrological context of any given storm event is likely to play a role in the sediment transport response as previous storms can either mobilize new sources or exhaust the supply of sediment flushed by runoff or within the channel (Gellis, 2013). For example, Li-qing et al. (2007) found that the magnitude of the first flush is not always correlated to maximum rainfall intensity, but is sensitive to the timing of maximum rainfall.

4.2. Trends in sediment and carbon load behavior

The shape of the relationship between discharge and *SS* indicates the relative availability of sediment among watersheds. Analyzing the 13 largest flow events, we found that mean hysteresis behavior was not significantly different among any pairs of watersheds. Thus the similar clockwise hysteresis patterns among watersheds were consistent with the hypothesis that sediment sources are similar among these watersheds. Generally, clockwise hysteresis represents a flushing of sediment prior to peak flow, indicating stream and bank storage of sediment and a limited sediment supply (Williams, 1989). Further, the log-log linear slopes of the discharge-sediment concentration lines were not significantly different among watersheds, suggesting similar sources of fine sediment from nearby channels and banks. While sediment may be supplied in small rills or gullies along the stream channel or from much greater distances in steeply sloped watersheds, frequent intense tropical storms produce runoff great enough to exhaust the supply of sediment. For example, when storm events were prolonged or followed previous storms in short succession, sediment supply was quickly exhausted in 'Uma'uma. Similar clockwise hysteresis trends were observed in high elevation, low-order streams of New Zealand, where McGlynn and McDonnell (2003) documented “carbon flushing” events as high fluxes of carbon prior to peak discharge followed by the dilution of carbon in the receding limb of the hydrograph. In general, this movement of sediment is an important carbon source to oceans (Carey et al., 2005), with catchment steepness, land-cover and soil erodibility important drivers of sediment yield (Dunne, 1979), variability that was minimized in this study. These results support the theory that steep gradient hillslopes and low-order streams result in high rates of physical weathering and limited sediment storage.

The transferability of conclusions at large (watershed) scales to small (plot/catchment) scales to understand the mechanisms driving soil erosion can be challenging owing to the non-linearity of runoff to soil erosion relationships (Benavides-Solorio and MacDonald, 2001; Strauch et al., 2016). Results are consistent with the global scale perspective of tropical rivers provided by Latrubesse et al. (2005) who found declining sediment yield with increasing mean annual discharge caused by natural thresholds within watersheds. During runoff events in short watersheds, allochthonous POC inputs dominate carbon export as light limitation and short transit time limits in situ carbon production. The transport of coarse woody debris and leaf litter across the landscape and in streams during runoff events is also likely to increase the availability of POC (Roberts et al., 2016). Using isotopic signatures, Komada et al. (2004) found POC exported in small mountainous rivers during flood events mainly consisted of surface soil, with limited rock-derived carbon.

4.3. Comparisons to sediment discharge on Pacific islands and other tropical watersheds

Results from this study are generally consistent with previous reports of sediment discharge from other Hawaiian watersheds (Table 9). Presley et al. (2008) examined sediment and nutrient fluxes in Waiakea Stream, also on the Island of Hawai'i, and reported annual sediment yields between 3.3 t km^{-2} and 5.8 t km^{-2}. On the Island of Oahu, Doty et al. (1981) calculated annual sediment yields for Kipapa and Moanalua streams of 124–617 t km^{-2} and 8.4–135 t km^{-2}, respectively. Stock and Tribble (2010) calculated total annual sediment yield for Kawela Watershed on Molokai at 357 t km^{-2} and for Hanalei Watershed on Kauai at 477 t km^{-2}. For the 'Uma'uma, Manowai'ōpae and Pāhale watersheds, total sediment yield for 2013 was 65 t km^{-2}, 172 t km^{-2}, and 324 t km^{-2}. Because total rainfall in 2013 was below average, estimated sediment yields are likely less than long-term values. Based on soil composition and conservation practices, El-Swaify et al. (1982) estimated a wide range of erosion rates for the Hamakua Coast of the Island of Hawai'i (0.0027–2.18 t km^{-2} yr^{-1}). Gaging stations in this study were located in forests above anthropogenic land-use impacts and also likely a conservative estimate of loads entering the ocean, as deforestation and agriculture typically increases sediment and carbon inputs to rivers (Schlesinger and Melack, 1981). In the upper reaches of a Costa Rican watershed, Krishnaswamy et al.

Table 9
Stream name, upstream catchment, island age, mean catchment slope (%), mean daily flow yield, mean daily runoff yield, mean and maximum daily suspended sediment yield for seven stations across four Hawaiian Islands.

Stream name	USGS Station #	Island	catchment (km^2)	Geologic age (my)	MAR (mm)	Mean catchment slope (%)	Median flow (m^3 s^{-1})	Mean (SE) daily sediment yield (t km^{-2})	Maximum daily sediment yield (t km^{-2})
'Uma'uma	–	Hawaii	74.427	0.011	4906	15.8	0.3370	3.67 (1.25)	619.7
Manowai'ōpae	–	Hawaii	3.836	0.011	4026	13.8	0.0020	0.51 (0.20)	88.3
Pāhale	–	Hawaii	10.143	0.011	4689	12.0	0.0000	2.41 (1.04)	529.8
Kawela	16,415,600	Molokai	13.675	1.5	1625	45.7	0.0000	0.88 (11.25)	285.9
N. Halawa	16,226,400	Oahu	11.914	3.0	2997	59.0	0.0000	0.44 (4.45)	127.2
Kamo'oali'i	16,272,200	Oahu	9.8937	2.5	2235	44.4	0.1982	0.26 (3.17)	126.5
Hanalei	16,103,000	Kauai	47.94	5.5	4750	62.6	3.4263	1.35 (10.98)	264.9

(2001) estimated sediment yields of 112 t km^{-2} yr^{-1}which increased to 404 t km^{-2} yr^{-1} at the ocean mouth.

Allochthonous carbon makes an important contribution to freshwater and nearshore tropical ecosystems (Atwood et al., 2012). Our estimates of POC in 2013 were within the range reported by Burns et al. (2001) for a watershed in tropical Papua New Guinea (2–5.8 t km^{-2} yr^{-1}) and reported for low-order streams in New Zealand (1.3 to 81 t km^{-2} yr^{-1}) by Carey et al. (2005). Further, Lyons (2002) measured yields as large as 168 t km^{-2} yr^{-1} POC for some high elevation, high rainfall watersheds. In drier tropical regions, forested catchments can lose as little as 20–30 t km^{-2} yr^{-1} whereas grazed catchments can lose as little as 100 t km^{-2} yr^{-1}and as much as 20,000 t km^{-2} yr^{-1}, depending on rainfall and slope (Dunne, 1979). Wiegner et al. (2009) demonstrated that storm flow conditions represent a 36–58 fold increase in POC over baseflows for the Wailuku River, on the Island of Hawai'i. Higher variability in streamflow represents increasing variability in runoff generation, which is expected to lead to greater transport of soil particulates in both sheets and rills.

The estimation of carbon loads from Hawaiian watersheds presented here only considered POC, but dissolved carbon (organic and inorganic) can comprise an even greater amount of carbon lost from terrestrial environments (Schlesinger and Melack, 1981; Zhu and Reed, 2012).While dissolved inorganic carbon (DIC), as the primary source of carbon for photosynthesis, is a strong influence on freshwater ecosystems, this represents a relatively small portion of the carbon pool in aquatic Hawaiian ecosystems (MacKenzie et al., 2017). Further, the fraction of suspended sediment that is particulate inorganic carbon (PIC) is minor (Wetzel, 2001) and chemical weathering of parent material is not enhanced by short-term pulses of runoff, with DIC usually diluted by high flow events (Komada et al., 2004).

4.4. Implications for watershed management

Land-cover change, including deforestation, invasion of non-native species, agricultural development, and urbanization can accelerate soil erosion, stream bank erosion, and sediment delivery, impairing freshwater (Wong and Yeatts, 2002; Allan, 2004; Strauch et al., 2016) and near-shore environments (Loya, 1976; Rogers, 1990; Storlazzi et al., 2009). The impairment of water resources by sediment is of critical concern to the State of Hawai'i as 86% of marine water bodies exceed water quality standards (State of Hawaii Department of Health, 2014). Sediment delivery negatively impacts marine ecosystems by damaging living coral tissues and preventing coral colonization (Howarth et al., 2000; Perez III et al., 2014). Impaired water resources threaten recreational water users, with substantial economic consequences (Flanders, 2007). Increased urbanization of coastal zones and channelization of streams in Hawai'i has reduced the area of salt marsh estuaries and wetlands that historically acted as natural filters before streamflow entered the near-shore (Van Rees and Reed, 2014).

Understanding the factors that influence sediment loads is important for generating reliable data for land and water management (Francke et al., 2008). In the tropics, rapid changes in *SS* during peak runoff events are likely to mask additional sediment loading due to landscape disturbance (Doty et al., 1981). Adding to this are the large natural variations in sediment loading and rainfall across space and time in young islands. In this model system, differences in watershed loading are primarily a function of the generation of runoff and the availability of sediment. Improving the protection of watersheds, particularly riparian vegetation and ground cover of steeply sloped regions, has been shown to help control erosion and sediment loads (Grace III, 2002; Strauch et al., 2016).

5. Conclusions

Anticipated shifts in the distribution and intensity of rainfall in tropical watersheds, including the length of drought between rainfall events, is expected to alter hydrological processes. Antecedent rainfall conditions and soil moisture influence the generation of runoff and the transport of sediment, with frequent rainfall events exhausting the supply of sediment in water logged soils. Attempts to model sediment and carbon fluxes with the LOADEST model have limited usefulness at short time steps because it poorly characterizes the high variability of tropical streamflow and therefore underestimated daily and annual values. Short-term events transport most of the sediment while accounting for only a small portion of the measurement period. Improvements in watershed management that protect riparian vegetation and promote native forest regeneration will help reduce sediment discharge to near-shore environments.

Acknowledgements

This work was supported by the University Hawai'i Mānoa Department of Natural Resources and Environmental Management and the USDA Forest Service Pacific Southwest Research Station Institute for Pacific Islands Forestry in Hilo, Hawai'i (Research Joint Venture #10-JV-11272177-030). We thank the support of T. Frauendorf, P. Folk, M. Roberts, T. Sowards, and R. Tingley III, for assistance with fieldwork and laboratory analysis. D. Karwan provided excellent comments on an earlier draft of this manuscript. We are grateful to Kamehameha Schools Bishop Estate for providing us access through their property.

References

Algeet-Abarquero, N., Marchamalo, M., Bonatti, J., Fernández-Moya, J., Moussa, R., 2015. Implications of land use change on runoff generation at the plot scale in the humid tropics of Costa Rica. Catena 135, 263–270.
Allan, J.D., 2004. Landscapes and riverscapes: the influence of land use on stream ecosystems. Annu. Rev. Ecol. Evol. Syst. 35, 257–284.
Allen, M.R., Ingram, W.J., 2002. Constraints on future changes in climate and the hydrologic cycle. Nature 419, 224–232.
Atwood, T.B., Wiegner, T.N., MacKenzie, R.A., 2012. Effects of hydrological forcing on the structure of a tropical estuarine food web. Oikos 121, 277–289.
Augustijn, D., Fares, A., Tran, D.N., 2011. Temporal and spatial variations in total suspended and dissolved solids in the upper part of Manoa stream, Hawaii. J. Sust. Water Sci. & Man 1, 1–9.
Barlage, M.J., Richards, P.L., Sousounis, P.J., Brenner, A.J., 2002. Impacts of climate change and land use change on runoff from a Great Lakes watershed. J. Great Lakes Res. 28, 568–582.
Benavides-Solorio, J., MacDonald, L.H., 2001. Post-fire runoff and erosion from simulated rainfall on small plots, Colorado Front Range. Hydrol. Process. 15, 2931–2952.
Brasington, J., Richards, K., 2000. Turbidity and suspended sediment dynamics in small catchments in the Nepal Middle Hills. Hydrol. Process. 14, 1559–2574.
Brooks, K.N., Ffolliott, P.F., Magner, J.A., 2013. Hydrology and the Management of Watersheds. Wiley-Blackwell, New York.
Burns, K.A., Hernes, P.J., Benner, R., Codi, S., Brinkman, D., 2001. Organic biomarkers aid in source function estimates for the Sepik River outflow into the New Guinea Coastal undercurrent. International Organic Geochemistry Meeting. European Association of Organic Geochemistry, Nancy, France.
Calhoun, R.S., Fletcher III, C.H., 1999. Measured and predicted sediment yield from a subtropical, heavy rainfall, steep-sided river basin: Hanalei, Kauai, Hawaiian Islands. Geomorphology 30, 213–226.
Campbell, J.L., Rustad, L.E., Boyer, E.W., Christopher, S.F., Driscoll, C.T., Fernandex, I.J., Groffman, P.M., Houle, D., Kiekbusch, J., Magill, A.H., Mitchell, M.J., Ollinger, S.V., 2009. Consequences of climate change for biogeochemical cycling in forests of northeastern North America. Can. J. For. Res. 39, 264–284.
Cao, G., Giambelluca, T.W., Stevens, D.E., Schroeder, T.A., 2007. Inversion variability in the Hawaiian trade wind regime. J. Clim. 20, 1145–1160.
Carey, A.E., Gardner, C.B., Goldsmith, S.T., Lyons, W.B., Hicks, D.M., 2005. Organic carbon yields from small, mountainous rivers, New Zealand. Geophys. Res. Lett. 32, L15404.
Chen, Y.R., Chu, P.-S., 2014. Trends in precipitation extremes and return levels in the Hawaiian Islands under a changing climate. Int. J. Climatol. 34, 3913–3925.
Chu, P.-S., Chen, H., 2005. Interannual and interdecadal rainfall variations in the Hawaiian islands. J. Clim. 18, 4796–4813.
Chu, P.-S., Chen, Y.R., Schroeder, T.A., 2010. Changes in precipitation extremes in the Hawaiian Islands in a warming climate. J. Clim. 23, 4881–4900.
Cuo, L., Giambelluca, T.W., Ziegler, A., Nullet, M., 2006. Use of the distributed hydrology soil vegetation model to study road effects on hydrological processes in Pang Khum Experimental Watershed, northern Thailand. For. Ecol. Manag. 224, 81–94.
Doty, R.D., Wood, H.B., Merriam, R.A., 1981. Suspended sediment production from forested watersheds on Oahu, Hawaii. Water Resour. Bull. 17, 399–404.
Dunne, T., 1979. Sediment yield and landuse in tropical catchments. J. Hydrol. 42, 281–300.
El-Swaify, S.A., Dangler, E.W., Armstrong, C.L., 1982. Soil erosion by water in the tropics. Research Extension Series 024. University of Hawaii, Honolulu, Hawaii, p. 173.

Fang, N.F., Shi, Z.H., Chen, F.X., Zhang, H.Y., Wang, Y.X., 2015. Discharge and suspended sediment patterns in a small mountainous watershed with widely distributed rock fragments. J. Hydrol. 528, 238–248.

Flanders, L.S., 2007. Recommendations for a State Management Plan at the Wai'Opae Tide Pools Kapoho, Hawaii. State of Hawaii Department of Land and Natural Resources, Honolulu, HI.

Francke, T., López-Tarazón, J., Schröderk, B., 2008. Estimation of suspended sediment concentration and yield using linear models, random forests and quantile regression forests. Hydrol. Process. 22, 4892–4904.

Frazier, A.G., Giambelluca, T.W., 2016. Spatial trend analysis of Hawaiian rainfall from 1920 to 2012. Int. J. Climatol. 37, 2522–2531.

Freeman, W., Fox, J., 1995. ALAWAT: a spatially allocated watershed model for approximating stream, sediment, and pollutant flows in Hawaii, USA. Environ. Manag. 19, 567–577.

Gellis, A.C., 2013. Factors influencing storm-generated suspended-sediment concentrations and loads in four basins of contrasting land use, humid-tropical Puerto Rico. Catena 104, 39–57.

Giambelluca, T.W., Chen, Q., Frazier, A.G., Price, J.P., Chen, Y.-L., Chu, P.-S., Eischeid, J.K., Delparte, D.M., 2013. Online rainfall atlas of Hawai'i. B. Am. Meteorol. Soc. 94, 313–316.

Giambelluca, T.W., Diaz, H.F., Luke, M.S.A., 2008. Secular temperature changes in Hawai'i. Geophys. Res. Lett. 35, L12702.

Grace III, J.M., 2002. Effectiveness of vegetation in erosion control from forest road sideslopes. T. ASAE 45, 681–685.

Grigg, R.W., 1995. Coral reefs in an urban embayment in Hawaii: a complex case history controlled by natural and anthropogenic stress. Coral Reefs 14, 253–266.

Holz, D.J., Williard, K.W.J., Edwards, P.J., Schoonover, J.E., 2015. Soil erosion in humid regions: a review. J. Contemp. Water Res. Educ. 154, 48–59.

Howarth, R., Andreson, D., Cloem, J., Elfring, C., Hopkinson, C., Lapointe, B., Malone, T., Marcus, N., McGlathery, K., Sharpley, A., Walker, D., 2000. Nutrient pollution of coastal rivers, bays and seas. Issues in Ecology 7, 1–15.

IPCC, 2013. Working Group I Contribution to the IPCC Fifth Assessment Report, Climate Change 2013: The Physical Science Basis. United Nations Environmental Program, Geneva.

Jennerjahn, T.C., Ittekkot, V., Klopper, S., Adi, S., Nugroho, S.P., Sudiana, N., Yusmal, A., Prihartant, Gaye-Haake, B., 2004. Biogeochemistry of a tropical river affected by human activities in its catchment: Brantas River estuary and coastal waters of Madura Strait, Java, Indonesia. Estuar. Coast. Shelf Sci. 60, 503–514.

Kleinman, P.J.A., Srinivasan, M.S., Dell, C.J., Schmidt, J.P., Sharpley, A.N., Bryant, R.B., 2006. Role of rainfall intensity and hydrology in nutrient transport via surface runoff. J. Environ. Qual. 35, 1248–1259.

Komada, T., Druffel, E.R.M., Trumbore, S.E., 2004. Oceanic export of relict carbon by small mountainous rivers. Geophys. Res. Lett. 31, L07504.

Krishnaswamy, J., Richter, D.D., Halpin, P.N., Hofmockel, M.S., 2001. Spatial patterns of suspended sediment yields in a humid tropical watershed in Costa Rica. Hydrol. Process. 15, 2237–2257.

Kurashige, Y., 1994. Mechanisms of sediment supply in headwater rivers. Japanese Geomorphological Union 15A, 109–129.

Latrubesse, E.M., Stevaux, J.C., Sinha, R., 2005. Tropical rivers. Geomorphology 70, 187–206.

Laws, E.A., Ferentinos, L., 2003. Human impacts on fluxes of nutrients and sediment in Waimanalo Stream, Oahu, Hawaiian Islands. Pac. Sci. 57, 119–140.

Lewis, J., 1996. Turbidity-controlled suspended sediment sampling for runoff-event load estimation. Water Resour. Res. 32, 2299–2310.

Lim, K.J., Engel, B.A., Tang, Z., Choi, J., Kim, K.-S., Muthukrishnan, S., Tripathy, D., 2005. Automated Web GIS based Hydrograph Analysis Tool, WHAT. J. Am. Water Res. Assoc. 41, 1407–1416.

Li-qing, L., Cheng-qing, Y., Qing-ci, H., Ling-li, K., 2007. First flush of storm runoff pollution from an urban catchment in China. J. Environ. Sci. 19, 295–299.

López-Tarazón, J.A., Batalla, R.J., Vericat, D., Balasch, J.C., 2010. Rainfall, runoff and sediment transport relations in a mesoscale mountainous catchment: the River Isábena (Ebro basin). Catena 82, 23–34.

Loya, Y., 1976. Effects of water turbidity and sedimentation on the community structure of Puerto Rican corals. B. Mar. Sci. 26, 405–466.

Lyons, W.B., Nezat, C.A., Carey, A.E., Hicks, D.M., 2002. Organic carbon fluxes to the ocean from high-standing islands. Geology 30, 443–446.

MacKenzie, R.A., Strauch, A.M., Wiegner, T.N., Colbert, S., Stets, E.G., Streigl, R.G., 2017. Baseline and projected future aquatic carbon fluxes to nearshore waters in Hawai'i. In: Selmants, P.C., Giardina, C.P., Jacobi, J.D., Zhu, Z. (Eds.), Baseline and Projected Future Aquatic Carbon Fluxes to Nearshore Waters in Hawai'i. 1834. U.S. Geological Survey Professional Paper, pp. 89–106.

McGlynn, B.L., McDonnell, J.J., 2003. Role of discrete landscape units in controlling catchment dissolved organic carbon dynamics. Water Resour. Res. 39, 1090.

McGregor, G.R., Nieuwolt, S., 1998. Tropical Climatology: An Introduction to the Climates of the Low Latitudes. 2nd ed. Wiley, New York, NY.

Meehl, G.A., 1996. Vulnerability of freshwater resources to climate change in the tropical Pacific region. Water Air Soil Pollut. 92, 203–213.

Millhous, R.T., 2003. Preliminary analysis of sediment transport capacity in the Colorado Plateau. Proceedings of Hydrology Days 1, 117–128.

Milly, P.C., Dunne, K.A., Vecchia, A.V., 2005. Global pattern of trends in streamflow and water availability in a changing climate. Nature 438, 347–350.

Mimura, N., Nurse, L., McLean, R., Agard, J., Briguglio, L., Lefale, P., Payet, R., Sem, G., 2007. Small Islands. In: Parry, M.L., Canziani, O.F., Palutikof, J.P., van der Linden, P.J., Hanson, C.E. (Eds.), Climate Change 2007: Impacts, Adaptation, and Vulnerability. Cambridge University Press, Cambridge, UK, pp. 688–716.

Muller, C.J., O'Gorman, P.A., Back, L.E., 2011. Intensification of precipitation extremes with warming in a cloud-resolving model. J. Clim. 24, 2784–2800.

Oki, D.S., 2004. Trends in streamflow characteristics at long-term gaging stations, Hawaii. U.S. Geological Survey Scientific Investigations Report 2004-5080, p. 120.

Olden, J.D., Poff, N.L., 2003. Redundancy and the choice of hydrologic indices for characterizing streamflow regimes. River Res. Appl. 19, 101–121.

Parham, J.E., Higashi, G.R., Lapp, E.K., Kuamoo, D.G.K., Nishimoto, R.T., Hau, S., Fitzsimons, J.M., Polhemus, D.A., Devick, W.S., 2008. Atlas of Hawaiian Watersheds & Their Aquatic Resources. State of Hawaii Department of Land and Natural Resources, Division of Aquatic Resources, Honolulu, HI.

Parry, M.L., Canziani, O.F., Palutikof, J.P., van der Linden, P.J., Hanson, C.E., 2007. Climate Change 2007: Impacts, Adaptation, and Vulnerability. Cambridge University Press, Cambridge, UK.

Perez III, K., Roderg, K.S., Jokiel, P.L., Lager, C.V., Lager, D.J., 2014. Effects of terrigenous sediment on settlement and survival of the reef coral *Pocillopora damicornis*. PeerJ 2, e387.

Polyakov, V., Fares, A., Kubo, D., Jacobi, J., Smith, C., 2007. Evaluation of a non-point source pollution model, AnnAGNPS, in a tropical watershed. Environ. Model. Softw. 22, 1617–1627.

Presley, T.K., Jamison, M.T.J., Nishimoto, D.C., 2008. Suspended-sediment and nutrient loads for Waiakea and Alenaio streams, Hilo, Hawaii, 2003–2006. U.S. Geological Survey Open-File Report 2007-1429, p. 73.

Roberts, M., Strauch, A.M., Wiegner, T., MacKenzie, R.A., 2016. Leaf litter breakdown of native and exotic tree species in two Hawaiian streams that differ in flow. Pac. Sci. 70, 209–222.

Rogers, C.S., 1990. Responses of coral reefs and reef organisms to sedimentation. Mar. Ecol. Prog. Ser. 62, 185–202.

Runkel, R.L., Crawford, C.G., Cohn, T.A., 2004. Load Estimator (LOADEST); a FORTRAN program for estimating constituent loads in streams and rivers. U.S. Geological Survey Techniques and Methods, p. 69.

Ruosteenoja, K., Carter, T.R., Jylhä, K., Tuomevirta, H., 2003. Future Climate in World Regions: An Intercomparision of Model-based Projections for the New IPCC Emissions Scenarios. Finnish Environment Institute, Helsinki, Finland, p. 644.

Safeeq, M., Fares, A., 2012. Hydrologic response of a Hawaiian watershed to future climate change scenarios. Hydrol. Process. 26, 2745–2764.

Schlesinger, W.H., Melack, J.M., 1981. Transport of organic carbon in the world's rivers. Tellus 33, 172–187.

Selmants, P.C., Giardina, C.P., Jacobi, J.D., Zhiliang, Z., 2017. Baseline and projected future carbon storage and carbon fluxes in ecosystems of Hawai'i. U.S. Geological Survey Professional Paper 1834:p. 134. https://doi.org/10.3133/pp1834.

Shanley, J.B., McDowell, W.H., Stallard, R.F., 2011. Long-term patterns and short-term dynamics of stream solutes and suspended sediment in a rapidly weathering tropical watershed. Water Resour. Res. 47, W07515.

Sherrod, D.R., Sinton, J.M., Watkins, S.E., Brunt, K.M., 2007. Geologic Map of the State of Hawaii. Honolulu, HI. U.S. Geological Survey Open-File Report 2007-1089.

Smith, H.G., Dragovich, D., 2009. Interpreting sediment delivery processes using suspended sediment-discharge hysteresis patterns from nested upland catchments, south-eastern Australia. Hydrol. Process. 23, 2415–2426.

State of Hawaii Department of Health, 2014. 2014 State of Hawaii Water Quality Monitoring and Assessment Report. State of Hawaii Department of Health, Honolulu, HI.

Stenback, G.A., Crumpton, W.G., Schilling, K.E., Helmers, M.J., 2011. Rating curve estimation of nutrient loads in Iowa rivers. J. Hydrol. 396, 158–169.

Stock, J., Tribble, G.W., 2010. Erosion and sediment loads from two Hawaiian watersheds. 2nd Joint Federal Interagency Conference, Las Vegas, NV. 27 June–1 July.

Storlazzi, C.D., Field, M.E., Bothner, M.H., Presto, M.K., Draut, A.E., 2009. Sedimentation processes in a coral reef embayment: Hanalei Bay, Kauai. Mar. Geol. 264, 140–151.

Strauch, A.M., 2017. Relative change in stream discharge from a tropical watershed improves predictions of fecal bacteria in near-shore environments. Hydrol. Sci. J. 62, 1381–1393.

Strauch, A.M., Bruland, G.L., MacKenzie, R.A., Giardina, C.P., 2016. Soil and hydrological responses to wild pig (*Sus scofa*) exclusion from native and strawberry guava (*Psidium cattleianum*)-invaded tropical montane wet forests. Geoderma 279, 53–60.

Strauch, A.M., Giardina, C.P., MacKenzie, R.A., Giambelluca, T.W., Heider, C., Salminen, E., Bruland, G.L., 2017. Modeled effects of climate change and plant invasion on watershed function across a steep tropical rainfall gradient. Ecosystems 20, 583–600.

Strauch, A.M., MacKenzie, R.A., Bruland, G.L., Giardina, C.P., 2015. Climate driven changes to rainfall and streamflow patterns in a model tropical island hydrological system. J. Hydrol. 523, 160–169.

Strauch, A.M., MacKenzie, R.A., Bruland, G.L., Tingley, R., Giardina, C.P., 2014. Climate change and land use drivers of fecal bacteria in tropical Hawaiian rivers. J. Environ. Qual. 43, 1475–1483.

Strauch, A.M., MacKenzie, R.A., Tingley III, R., 2017. Base flow driven shifts in tropical stream temperature regimes across a mean annual rainfall gradient. Hydrol. Process. 31, 1678–1689.

Syvitski, J.P.M., Cohen, S., Kettner, A.J., Brakenridge, G.R., 2014. How important and different are tropical rivers? – an overview. Geomorphology 227, 5–17.

Syvitski, J.P.M., Peckham, S.D., Hilberman, R., Mulder, T., 2003. Predicting the terrestrial flux of sediment to the global ocean: a planetary perspective. Sediment. Geol. 162, 5–24.

Timm, O., Diaz, H.F., Giambelluca, T.W., Takahashi, M., 2011. Projection of changes in the frequency of heavy rain events over Hawai'i based on leading Pacific climate models. J. Geophys. Res. 116, D04109.

Timm, O., Takahashi, M., Giambelluca, T.W., Diaz, H.F., 2013. On the relation between large-scale circulation pattern and heavy rain events over the Hawaiian Islands: recent trends and future changes. J. Geophys. Res.-Atmos. 118, 4129–4141.

Torri, D., Sfalanga, M., Chisci, G., 1987. Threshold conditions for incipient rilling. Catena 8, 97–107.

USDA, 2008. Soil Survey Geographic (SSURGO) Database for Island of Hawaii Area, Hawaii. (Available at: http://SoilDataMart.nrcs.usda.gov/ (Accessed 2012)).

Van Rees, C., Reed, J.M., 2014. Wetland loss in Hawaii since human settlement. Wetlands 34, 335–350.
Victor, S., Neth, L., Golbuu, Y., Wolanski, E., Richmond, R.H., 2006. Sedimentation in mangroves and coral reefs in a wet tropical island, Pohnpei, Micronesia. Estuar. Coast. Shelf Sci. 66, 409–416.
Vitousek, P.M., 1995. The Hawaiian Islands as a model system for ecosystem studies. Pac. Sci. 49, 2–16.
Vitousek, P.M., Chadwick, O.A., Matson, P.A., Allison, S., Derry, L., Kettley, L., Luers, A., Mecking, E., Monastra, V., Porder, S., 2003. Erosion and the rejuvenation of weathering-derived nutrient supply in an old tropical landscape. Ecosystems 6, 762–772.
Walling, D.E., 1977. Assessing the accuracy of suspended sediment rating curves for a small basin. Water Resour. Res. 13, 531–538.
Webster, P.J., Holland, G.J., Curry, J.A., Chang, H.-R., 2005. Changes in tropical cyclone number, duration, and intensity in a warming environment. Science 309, 1844–1846.
Wetzel, R.G., 2001. Limnology: Lake and River Ecosystems. 3rd ed. Academic Press, Boston, USA.
Wiegner, T.N., Tubal, R.L., MacKenzie, R.A., 2009. Bioavailability and export of dissolved organic matter from a tropical river during base- and stormflow conditions. Limnol. Oceanogr. 54, 1233–1242.
Williams, G.P., 1989. Sediment concentration versus water discharge during single hydrologic events in rivers. J. Hydrol. 111, 89–106.
Wohl, E., Barros, A., Brunsell, N., Chappell, N.A., Coe, M.T., Giambelluca, T.W., Goldsmith, S., Harmon, R., Hendrickx, J.M.H., Juvik, J.O., McDonnell, J., Ogden, F., 2012. The hydrology of the humid tropics. Nat. Clim. Chang. 2, 655–662.
Wong, M.F., Yeatts, D.S., 2002. Streamflow and suspended-sediment loads before, during, and after H-3 highway construction, North Halawa, Haiku, South Fork Kapunahala, and Kamooalii drainage basins, Oahu, Hawaii, 1983-99. U.S. Geological Survey Water Resources Investigations 2002-4005.
Yuan, Y., Jiang, Y., Taguas, E.V., Mbonimpa, E.G., Hu, W., 2015. Sediment loss and its cause in Puerto Rico watersheds. Soil 1, 595–602.
Zhu, Z., Reed, B.C., 2012. Baseline and projected future carbon storage and greenhouse-gas fluxes in ecosystems of the Western United States. U.S. Geological Survey Professional Paper 1797, p. 192.